

LETTER TO THE EDITOR

# Discovery of an extremely bright submillimeter galaxy at $z=3.93$

J.-F. Lestrade<sup>1</sup>, F. Combes<sup>1</sup>, P. Salomé<sup>1</sup>, A. Omont<sup>2</sup>, F. Bertoldi<sup>3</sup>, P. André<sup>4</sup>, and N. Schneider<sup>4</sup>

<sup>1</sup> Observatoire de Paris, LERMA, CNRS, 61 Av. de l'Observatoire, F-75014, Paris, France

<sup>2</sup> Institut d'Astrophysique de Paris, UMR 7095, CNRS, UPMC Univ. Paris 06, 98bis Boulevard Arago, F-75014, Paris, France

<sup>3</sup> Argelander Institute for Astronomy, University of Bonn, Auf dem Hügel 71, 53121 Bonn, Germany

<sup>4</sup> Laboratoire AIM Paris-Saclay, CEA/IRFU/SAP - CNRS -, Université Paris Diderot, 91191 Gif-sur-Yvette Cedex, France

Received 2 September 2010; accepted 13 October 2010

## ABSTRACT

Serendipitously we have discovered a rare, bright submillimeter galaxy (SMG) with a flux density of  $30 \pm 2$  mJy at  $\lambda = 1.2$ mm, using MAMBO2 at the IRAM 30-meter millimeter telescope. Although no optical counterpart is known for MM18423+5938, we were able to measure the redshift  $z = 3.92960 \pm 0.00013$  from the detection of CO lines using the IRAM Eight Mixer Receiver (EMIR). In addition, by collecting all available photometric data in the far-infrared and radio to constrain its spectral energy distribution, we derive the FIR luminosity  $4.8 \cdot 10^{14} / m L_{\odot}$  and mass  $6.0 \cdot 10^9 / m M_{\odot}$  for its dust, allowing for a magnification factor  $m$  caused by a probable gravitational lens. The corresponding star-formation rate is  $8.3 \cdot 10^4 / m M_{\odot}/\text{yr}$ . The detection of three lines of the CO rotational ladder, and a significant upper limit for a fourth CO line, allow us to estimate an  $H_2$  mass of between  $1.9 \cdot 10^{11} / m M_{\odot}$  and  $1.1 \cdot 10^{12} / m M_{\odot}$ . The two lines  $C\text{I}(\overset{3}{P}_1 - \overset{3}{P}_0)$  and  $C\text{I}(\overset{3}{P}_2 - \overset{3}{P}_1)$  were clearly detected and yield a  $[C\text{I}]/[H_2]$  number abundance of between  $1.4 \cdot 10^{-5}$  and  $8.0 \cdot 10^{-5}$ . Upper limits are presented for emission lines of HCN,  $HCO^+$ , HNC,  $H_2O$ , and of other molecules. The moderate excitation of the CO lines is indicative of an extended starburst, and excludes the dominance of an AGN in heating this high- $z$  SMG.

**Key words.** Galaxies: evolution - Galaxies: high-redshift - Galaxies: ISM - Infrared: galaxies - Submillimeter: galaxies

## 1. Introduction

Deep blank-field millimeter and submillimeter surveys of small fields ( $\sim 1 \text{ deg}^2$ ) have revealed many dusty, starburst submillimeter galaxies (SMGs) over the past decade with flux densities of a few to about ten mJy at  $\lambda = 1.2$ mm (e.g. Bertoldi et al. 2007, Greve et al. 2008), and higher at  $\lambda = 850\mu\text{m}$  owing to dust emissivity (e.g. Smail et al. 1997). Recently, the South Pole Telescope survey, less deep but much larger in sky coverage ( $87 \text{ deg}^2$ ), has found 47 brighter SMGs with flux densities between 11 and 65 mJy at  $\lambda = 1.4$ mm (Vieira et al. 2010). Whereas redshifts of SMGs are crucial to study their physical properties, most of these dust-obscured galaxies have very faint or no optical counterparts, making measurements of spectroscopic redshift extremely difficult or impossible (e.g. Smail et al. 2002).

These dust-enshrouded star-forming galaxies are expected to be at high redshifts and are identified with the most massive galaxies assembled during an energetic early phase of galaxy formation. Their abundance appears to peak at  $z \sim 2.5$  (Chapman et al. 2005, Wardlow et al. 2010). Their star formation rate is prodigious at up to  $10^3 M_{\odot}\text{yr}^{-1}$ , and the underlying starburst activity is believed to result from mergers (Blain et al. 2002).

Lestrade et al. (2009) discovered serendipitously a rare, bright point source, MM18423+5938, at  $\lambda = 1.2$ mm (30 mJy) by mapping 50 separate fields totalling a sky area of  $0.5 \text{ deg}^2$  with the MAMBO2 bolometer camera (Kreysa et al. at the IRAM 30-meter millimeter telescope). Subsequently, some of us (PA and NS) searched but did not find local CO in the direction of the source suggesting not a young stellar object but an SMG instead, despite the Vieira et al.'s cumulative source count that

yields a chance as low as  $\sim 7\%$  of finding a 30mJy SMG. MM18423+5938 is detected at  $70 \mu\text{m}$  but undetected at  $24 \mu\text{m}$  in MIPS/Spitzer images. It is in neither the 2MASS catalogue, nor the NVSS VLA catalogue ( $S_{1.4\text{GHz}} < 2.5\text{mJy}$ ), and no optical and X-ray identifications are found in catalogues searched with NED (MM18423+593 is however outside the SDSS footprint). All these photometric data are summarized in Table 1.

We show in this Letter that MM18423+5938 is a bright, high-redshift SMG. We present in Sect. 2 our IRAM/EMIR spectroscopic observations of MM18423+5938 at millimeter wavelengths that yielded our detections of CO and C I, and upper limits for other molecular species. In Sect. 3, we model the data to infer the dust and gas content of MM18423+5938 and its general properties. To compute distances and luminosities, we adopt the  $\Lambda$ -CDM concordance cosmological model,  $H_0 = 71 \text{ km/s/Mpc}$ ,  $\Omega_M = 0.27$ , and  $\Omega_{\Lambda} = 0.73$  (Hinshaw et al. 2009).

## 2. Observations and data analysis

Lestrade et al. (2009) detected MM18423+5938 with a high but uncertain integrated flux density of  $30 - 60$  mJy, given that it was located close to the border of their MAMBO map. We reobserved MM18423+5938 with MAMBO at the IRAM 30-m telescope in the on-off wobbler-switching mode on 2010 January 16 using the map coordinates ( $\alpha_{2000} = 18^{\text{h}}42^{\text{m}}22.5^{\text{s}} \pm 0.2^{\text{s}}$  and  $\delta_{2000} = 59^{\circ}38'30'' \pm 2''$ ) and measured  $30 \pm 2$  mJy at  $\lambda = 1.2$ mm.

MM18423+5938 is located close to the border of the archived MIPS/Spitzer maps centered on the star GJ725AB (AOR 4199424). We determined the flux densities of the star GJ725AB and MM18423+5938 at  $70 \mu\text{m}$  and  $24 \mu\text{m}$  by means of aperture photometry, scaling with the stellar photospheric flux densities of GJ725AB predicted by the NextGen stellar atmo-

Send offprint requests to: J.-F. Lestrade, e-mail: jean-francois.lestrade@obspm.fr

arXiv:1009.0449v2 [astro-ph.CO] 15 Oct 2010

spheric model (Allard et al. 2001). We note a difference of  $9''$ , *i.e.* at the  $3\sigma$  level, between the positions of the source in our MAMBO map (Lestrade et al. 2009) and the archived  $70\ \mu\text{m}$  MIPS Spitzer map, which is not understood.

To measure the redshift of MM18423+5938, we used the strategy of observation developed by Weiss et al. (2009) with the multi-band heterodyne receiver Eight MIXer Receiver (EMIR<sup>1</sup>) at the IRAM 30-m telescope. The 3mm setup (E090) of EMIR provides 7.43 GHz of instantaneous, dual linear polarization bandwidth. The entire frequency range from 77.7 to 115.8 GHz in the 3mm band can be searched with six tunings spaced to provide 0.5 GHz overlap. This range corresponds to  $0 < z < 0.48$  and  $1 < z < 10$  for the CO lines between ( $J=1-0$ ) and ( $J=8-7$ ). Observations were conducted from 2010 July 29th to August 2nd with precipitable water vapor comprised between 3 and 7mm and with standard system temperatures of 110K for the E090 setup. Data were processed with 16 units of the Wide band Line Multiple Autocorrelator (WILMA) providing a spectral resolution of 2 MHz for the E090 setup. The observations were conducted in wobbler-switching mode, with a switching frequency of 1 Hz and an azimuthal wobbler throw of  $100''$ . Pointing and focus offsets were determined once every two hours and found to be stable. Calibration was done every 6 minutes using the standard hot/cold load absorber. The data were reduced with the CLASS software.

<sup>1</sup> <http://www.iram.es/IRAMES/mainWiki/EmirforAstronomers>

**Table 1.** Photometry available for MM18423+5938

Band	$S_\nu$ (mJy)	Ref
1.4 GHz	$< 2.5$	NVSS
3 mm	$2^{+2.0}_{-1.5}$	this work
2 mm	$9 \pm 3$	this work
1.2 mm	$30 \pm 2$	this work
$100\ \mu\text{m}$	$< 600$	IRAS
$60\ \mu\text{m}$	$< 100$	IRAS
$70\ \mu\text{m}$	$31 \pm 4$	Spitzer/MIPS
$24\ \mu\text{m}$	$< 0.6$	Spitzer/MIPS
B V R I	B mag $> 21$	NED (DSS)

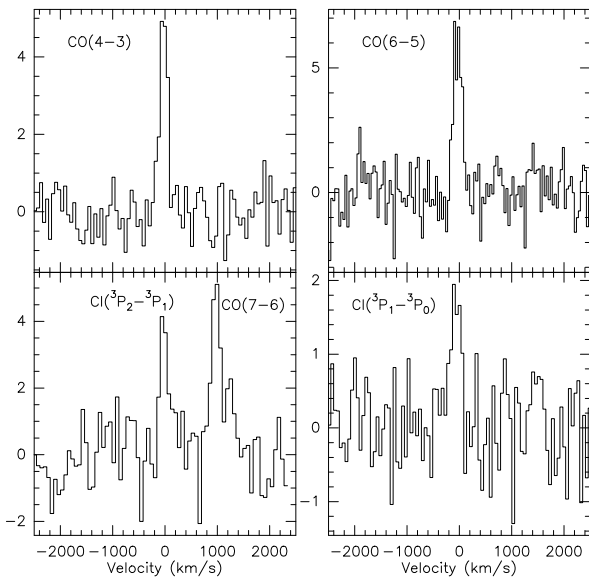


**Fig. 1.** The three CO rotational lines detected, and the two C I lines. The vertical scale is  $T_{mb}$  in mK.

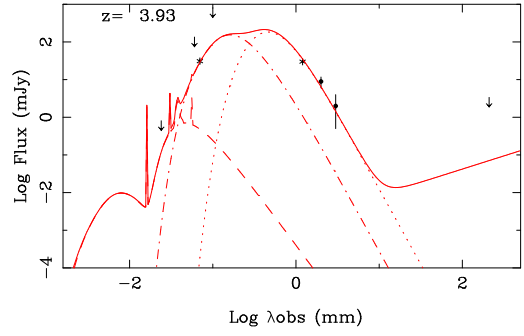


**Fig. 2.** Available photometric data for MM18423+5938 (Table 1). These are superimposed upon our dust emission model (full red curve) based on the Milky Way dust model by Desert et al (1990) adapted for our source at  $z=3.93$ . It consists of three components ; the large grains at  $T_d=45\text{K}$ , containing most of the mass (dotted line), the very small grains at hotter temperature (dot-dash), and the PAH (dashed line).

We started to scan the whole 3mm band by integrating data for  $\sim 2$  hrs for each tuning. We discovered unambiguously a line at 93.52 GHz after 20 minutes of integration during our third tuning on the second night, and continued to integrate dual polarisation data for 1.5 hr in total to reach an rms noise level of  $T_{mb}=0.8\ \text{mK}$  in  $60\ \text{km s}^{-1}$  channels (Fig 1 lefthand top panel). At this stage, we successively assumed that this line could be CO(1-0), CO(2-1), ... to calculate for each of these assumptions the corresponding redshift and predict the frequencies of the higher  $J$  transitions accessible in the 2mm band of EMIR (setup E150 from 127 to 176 GHz). We then tuned to these frequencies with the E150 setup and swiftly detected a line at 140.26 GHz that corresponds to CO(6-5) at  $z = 3.92960 \pm 0.00013$ , in addition to the line at 93.52 GHz for CO(4-3). This identification of the CO transitions and determination of the redshift of MM18423+5938 were carried out during the same night of July 30/31 in  $\sim 6$  hours. The rest of the allocated time (15 hours) was used to search for CO(7-6) (detected), CO(9-8) (undetected, consequently CO(10-9) was not searched), and for other species, C I (two lines detected), and HCN & HNC(5-4), LiH(1-0) & HCO+(5-4),  $\text{H}_2\text{O}_o$ ,  $\text{H}_2\text{O}_p$ ,  $^{13}\text{CO}(5-4)$ , CS(8-7), and CS(9-8) (all undetected but interesting upper limits are discussed below, see Table 3). Two CO lines (5-4 and 8-7) unfortunately are in the atmospheric  $\text{O}_2$  and  $\text{H}_2\text{O}$  lines opacity domains and could not be observed. The spectra were of high quality, stable, and flat. Their mean levels measure the continuum flux densities at 2mm and 3mm (Table 1) owing to the excellent weather conditions (precipitable water vapor  $\sim 4\ \text{mm}$ ).

Figure 1 displays the three CO lines detected, along with the two C I lines. Spectra were smoothed to a resolution of 30-50 km/s. Gaussian models were fitted to the lines and the results are reported in Table 2. Line widths found are normal *albeit* small suggesting that we are observing a galaxy seen rather face-on.

### 3. Results

#### 3.1. Dust emission

The photometric data are collected in Table 1. To model these data in Fig. 2, we choose to use the well-established Milky Way dust model of Desert et al (1990) as a template. This model consists of three main components, PAH and both very small and large grains, and the emissivity slope is assumed to be  $\beta=2$ . The large dust grains are dominant in mass and their tempera-

**Table 2.** Observed line parameters

Line	$\nu_{\text{obs}}$ [GHz]	$T_{\text{mb}}$ [mK]	$S_{\nu}$ [mJy]	$\Delta V_{\text{FWHM}}$ [km s $^{-1}$ ]	$I$ [Jy km s $^{-1}$ ]	$V^*$ [km s $^{-1}$ ]	$L'/m/10^{10}$ [K km s $^{-1}$ pc $^2$ ]
CO(4-3)	93.5249	$5.3 \pm 0.6$	$26.7 \pm 3.$	$175 \pm 20$	$4.95 \pm 0.5$	$0 \pm 8$	$19.7 \pm 2.$
CO(6-5)	140.2695	$6.4 \pm 1$	$32.8 \pm 5.$	$189 \pm 19$	$6.6 \pm 0.6$	$-7 \pm 9$	$11.5 \pm 1.$
CO(7-6)	163.6342	$4.2 \pm 0.9$	$21.5 \pm 4.6$	$172 \pm 27$	$3.9 \pm 0.5$	$11 \pm 11$	$5.0 \pm 0.6$
C I( $^3P_1-\tilde{P}_0$ )	99.8378	$1.9 \pm 0.6$	$9.6 \pm 3.$	$225 \pm 55$	$2.3 \pm 0.5$	$-50 \pm 24$	$8.0 \pm 1.7$
C I( $^3P_2-\tilde{P}_1$ )	164.1802	$4.2 \pm 1.$	$21.5 \pm 5.$	$184 \pm 49$	$4.2 \pm 0.8$	$8 \pm 19$	$5.3 \pm 1.$

Quoted errors are statistical errors from Gaussian fits. The systematic calibration uncertainty is 10%

\* The velocity is given relative to  $z=3.929605$ .

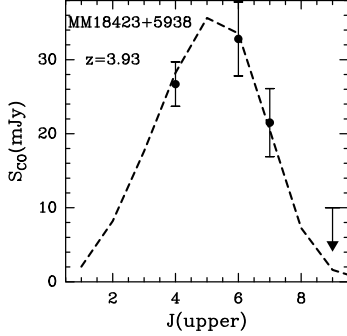


**Fig. 3.** CO line flux density (points) or upper limits (arrow) measured at the IRAM-30m, with the best-fit LVG model (dashed line) computed with a density  $n_{\text{H}_2} = 10^3 \text{ cm}^{-3}$ ,  $T_k = 45\text{K}$ , and  $N_{\text{CO}}/\Delta V = 3 \cdot 10^{18} \text{ cm}^{-2}/\text{km s}^{-1}$ .

ture is estimated to be  $T_d = 45\text{K}$ , constrained by the Rayleigh-Jeans part of the emission. The very small grains are made of two temperature components,  $\sim 80$  and  $\sim 130\text{K}$ , constrained by the  $70\mu\text{m}$  Spitzer measurement and the robust relationship between  $L'_{\text{CO}(3-2)}$  and  $L_{\text{FIR}}$  found by Iono et al (2009). A single temperature component for the small grains in the model was tried but the resulting  $L_{\text{FIR}}$  is significantly inconsistent with this relationship. The total mass of the dust required by this model is  $M_{\text{dust}} = 6.0 \cdot 10^9 / m M_{\odot}$ , and for a gas-to-dust mass ratio of 150, we infer that  $M_{\text{gas}} = 9.2 \cdot 10^{11} / m M_{\odot}$ . We suspect there is a gravitational lens along the line of sight, with an amplification factor  $m$ , or these values would be implausibly at least one order of magnitude larger than for rare hyperluminous objects. We derive the total FIR luminosity  $L_{\text{FIR}} = 4.8 \cdot 10^{14} / m L_{\odot}$  and the star-formation rate  $\text{SFR} = 8.3 \cdot 10^4 / m M_{\odot}/\text{yr}$ , by applying the relation of Kennicutt (1998).

### 3.2. CO lines

The CO SED of MM18423+5938 in Fig. 3 indicates moderate line excitation, peaking only at  $J=5$ ; CO SEDs peak at  $J=6$  or  $7$  in local starbursts such as M82 and NGC253 (Weiss et al 2007), peak at higher  $J$  in AGN-dominated sources, e.g.  $J=10$  in APM0827, and reach a plateau for  $J > 8$  in Mrk231 (van der Werf et al 2010). We ran several LVG models, to constrain the  $\text{H}_2$  volumic density and the kinetic temperature (cf Combes et al 1999). The moderate excitation implies a regime of low temperature and/or density. The gas kinetic temperature is taken to be equal to the dust temperature ( $T_d=45\text{K}$ ). When models are run with higher  $T_k$ , they all imply  $n(\text{H}_2)$  lower than  $10^3 \text{ cm}^{-3}$ , which is not realistic for CO(7-6)-emitting clouds. Our estimate

is therefore  $T_k=45\text{K}$ ,  $n(\text{H}_2)=10^3 \text{ cm}^{-3}$ , and a column density per velocity interval  $N_{\text{CO}}/\Delta V = 3 \cdot 10^{18} \text{ cm}^{-2}/\text{km s}^{-1}$ , as adopted to model the data in Figure 3. From the CO(1-0) line derived from our LVG model, we infer an  $\text{H}_2$  mass of  $1.9 \cdot 10^{11} / m M_{\odot}$  with the conversion factor  $M(\text{H}_2)/L'_{\text{CO}} = 0.8 M_{\odot}/(\text{K km s}^{-1} \text{ pc}^2)$  adopted for ULIRGs by Solomon et al (1997). This latter value yields a lower limit, while the standard conversion ratio for the Milky Way, 5.75 times higher, yields the upper limit  $M(\text{H}_2) = 1.1 \cdot 10^{12} / m M_{\odot}$ . The true mass must lie between these two values, and indicates large amounts of molecular gas even if allowing for an amplification  $m$ . Assuming a typical intrinsic extension of  $3\text{kpc}$  (e.g. Tacconi et al 2006), the surface filling factor of the molecular component is 0.3 for  $m=1$ , and 0.03 for  $m=10$ . The  $L_{\text{FIR}}/L'_{\text{CO}}$  of  $2 \cdot 10^3 L_{\odot}/\text{K km s}^{-1} \text{ pc}^2$  is consistent with ratios of other luminous infrared galaxies within the scatter (Iono et al 2009).

### 3.3. Atomic carbon lines

The two lines C I( $^3P_1-\tilde{P}_0$ ) and C I( $^3P_2-\tilde{P}_1$ ) were clearly detected. They have comparable central velocity and line width (Table 2), implying that they originate from the same region in the source. The relation between the integrated C I( $^3P_1-\tilde{P}_0$ ) brightness temperature and the beam averaged C I column density with the usual assumption of the optically thin limit is given by

$$N_{\text{CI}} = \frac{8\pi k \nu_{10}^2}{hc^3 A_{10}} Q(T_{\text{ex}}) \frac{1}{3} e^{T_1/T_{\text{ex}}} \int T_{\text{mb}} dv,$$

where  $Q(T_{\text{ex}}) = 1 + 3e^{-T_1/T_{\text{ex}}} + 5e^{-T_2/T_{\text{ex}}}$  is the C I partition function, and  $T_1 = 23.6 \text{ K}$  and  $T_2 = 62.5 \text{ K}$  are the energies above the ground state. When dealing with high- $z$  sources, we can use the definition of the line luminosity (e.g. Solomon et al. 1997) and derive the C I mass via (cf Weiss et al 2003, 2005)

$$M_{\text{CI}} = 1.902 \times 10^{-4} Q(T_{\text{ex}}) e^{23.6/T_{\text{ex}}} L'_{\text{CI}(^3P_1-\tilde{P}_0)} [M_{\odot}].$$

The mass estimated from the higher-excitation line is expressed in an analogous way, and we can then deduce that

$$\frac{L'_{\text{CI}(^3P_2-\tilde{P}_1)}}{L'_{\text{CI}(^3P_1-\tilde{P}_0)}} = 2.087 e^{-38.9/T_{\text{ex}}},$$

where line luminosities are given in Table 2. The derived  $T_{\text{ex}}$  is  $33.9 \text{ K}$ . The mass of atomic carbon thus amounts to  $M_{\text{CI}} = 1.0 \cdot 10^8 / m M_{\odot}$ . Given our lower and upper limits to the  $\text{H}_2$  mass from the CO lines, the  $[\text{C I}]/[\text{H}_2]$  number abundance is between  $1.4 \cdot 10^{-5}$  and  $8.0 \cdot 10^{-5}$ . This is somewhat higher than the average  $[\text{C I}]/[\text{H}_2]$  number abundance found in comparable star-forming objects (e.g. Barvainis et al 1997, Pety et al 2004, Weiss

**Table 3.** Line upper limits

Line	$\nu_{obs}$ [GHz]	$S_{\nu}(3\sigma)$ [mJy]	$L'/10^{10}$ [K km s <sup>-1</sup> pc <sup>2</sup> ]
CO(9-8)	210.344	< 10.	<1.4
<sup>13</sup> CO(4-3)	89.412	< 10.	<8.1
HCN& HNC(5-4)	90.	< 7.	<5.5
LiH(1-0) & HCO+(5-4)	90.	< 7.	<5.5
H <sub>2</sub> O <sub>v</sub> (1,1,0-1,0,1)	112.978	< 10.	<5.0
H <sub>2</sub> O <sub>p</sub> (2,1,1-2,0,2)	152.554	< 12.	<3.3
CS(8-7)	79.488	< 11.	<11.2
CS(9-8)	89.420	< 7.	<5.6

et al 2003, 2005, Riechers et al 2009, Danielson et al. 2010). In these latter estimates, although the observed  $L_{CI}/L_{CO}$  values are comparable, the  $[C\ I]/[H_2]$  number abundances are somewhat dissimilar because of the various CO-to-H<sub>2</sub> conversion factors adopted by these authors. Abundance lower than  $1.8 \cdot 10^{-5}$  has been reported (Casey et al 2010). The contribution of the atomic carbon to the cooling is low,  $L_{CI}/L_{FIR} = 2.5 \cdot 10^{-6}$ , comparable to that of nearby star-forming galaxies (Gerin & Phillips 2000).

### 3.4. Other lines

We searched for high-density tracers, such as HCN, HNC, and HCO<sup>+</sup>, in particular their lowest level available, i.e. J=5-4. The upper limits found (Table 3) confirm that, on average, the H<sub>2</sub> density is not high, as found by our LVG models of the CO line excitation. The HCN luminosity is higher than one third of the CO luminosity in local AGN-dominated objects (Imanishi et al 2004), and we note that our  $3\sigma$  upper limit ( $L'_{HCN(5-4)}/L'_{CO(5-4)} \sim 0.28$ ) is close to this limit. However, observation of HCN(1-0) and CO(1-0) are needed to conclude.

We also searched for H<sub>2</sub>O emission, using the first ortho and para lines in their ground states, i.e. H<sub>2</sub>O( $J_{K_a K_c}=1_{10} \rightarrow 1_{01}$ ) and H<sub>2</sub>O( $J_{K_a K_c}=2_{11} \rightarrow 2_{02}$ ) but only obtained interesting upper limits. Assuming that these water lines are optically thick, these upper limits yield a filling factor of dense clumps lower than 30% that of CO clouds.

At  $z=2.3$ , a tentative detection of the H<sub>2</sub>O( $J_{K_a K_c}=2_{11} \rightarrow 2_{02}$ ) line was reported in IRAS F10214 (Encrenaz et al. 1993; Casoli et al. 1994), while at  $z=0.685$ , the fundamental transition of ortho-water, H<sub>2</sub>O( $J_{K_a K_c}=1_{10} \rightarrow 1_{01}$ ), was detected in absorption towards B0218+357 (Combes & Wiklind 1997). Water lines were searched for other starburst galaxies at high  $z$  (Riechers et al., 2006, Wagg et al. 2006), and significant upper limits set. A search for H<sub>2</sub>O( $J_{K_a K_c}=1_{10} \rightarrow 1_{01}$ ) emission toward the  $z=3.91$  quasar APM 08279+5255 provided a surface-filling factor lower than 12% of the CO one (Wagg et al. 2006, Weiss et al. 2007).

Finally, other interesting molecules were undetected in the observed bands, although with insufficient sensitivity: <sup>13</sup>CO(4-3) (limiting the <sup>13</sup>CO/<sup>12</sup>CO emission ratio to < 1/2), CS(8-7), LiH (1-0) lines, several lines of formaldehyde H<sub>2</sub>CO, and SiO, which is a tracer of shocks. Their lowest transitions observed are H<sub>2</sub>CO(7(2, 5) - 8(0, 8)), H<sub>2</sub>CO(6(1, 6) - 5(1, 5)), SiO(9-8) and upper limits are  $L' < 20 \cdot 10^{10}$  K km s<sup>-1</sup> pc<sup>2</sup>.

## 4. Discussion and conclusion

We have found that the brightest SMG in the North, MM18423+5938, is at a redshift  $z = 3.92960 \pm 0.00013$ . This source is part of a most interesting population of similar ob-

jects recently found by the Herschel Atlas survey (Negrello et al 2010 submitted). From our modelled SED, the FIR luminosity  $4.8 \cdot 10^{14}/m L_{\odot}$  and mass  $6.0 \cdot 10^9/m M_{\odot}$  for the dust of MM18423+5938, and the implied star-formation rate of  $8.3 \cdot 10^4/m M_{\odot}/yr$ , lead to suspect a gravitational lens along the line of sight with an amplification factor  $m$ . From our modelled CO SED, we have found that  $M(H_2)$  is between 1.9 and  $10.8 \cdot 10^{11}/m M_{\odot}$  depending on the conversion ratio, indicating large amounts of molecular gas. The CO line excitation is moderate which indicates that there is both no strong heating by a central AGN and a starburst that is not too extreme. The average density of the molecular medium is low, of the order of  $10^3$  cm<sup>-3</sup>, and the gas kinetic temperature is assumed to be 45K in our model. The atomic carbon lines, assumed optically thin, are excited to  $T_{ex} = 33.9K$  and yield  $M_{CI}=1.0 \cdot 10^8/m M_{\odot}$ , which corresponds to a  $[C\ I]/[H_2]$  number abundance of between  $1.4 \cdot 10^{-5}$  and  $8.0 \cdot 10^{-5}$  when the limits on the H<sub>2</sub> mass derived from the CO lines are used. In this high- $z$  SMG, the C I-to-CO luminosity ratio is consistent with those of other high- $z$  galaxies.

The moderate CO line excitation found excludes a dominant AGN in MM18423+5938, unlike Mrk231 where CO is excited up to J=13 (van der Werf et al 2010). This moderate excitation favors an extended gas disk (typically 3kpc), rather than a compact nuclear starburst (300pc) and consequently a high CO-to-H<sub>2</sub> conversion ratio. This high-redshift SMG, with a star formation efficiency of  $L_{FIR}/L'_{CO}=2400$ , is comparable to the lower- $z$  submillimeter galaxies studied by Greve et al (2005).

*Acknowledgements.* Based on observations carried out with the IRAM 30m telescope. IRAM is supported by INSU/CNRS (France), MPG (Germany) and IGN (Spain). The authors are grateful to the IRAM staff for their support, and to the referee for helpful comments.

## References

- Allard, F., Hauschildt, P. H., Alexander, D. R., et al., 2001, ApJ, 556, 357  
 Bertoldi, F., Carilli C., Aravena M. et al, 2007, ApJSS, 172, 132  
 Blain A.W., Smail I., Ivison R.J. et al. 2002, PhR, 369, 111  
 Casey C.M., Chapman S.C., Daddi E. et al.: 2009, MNRAS 400, 670  
 Casoli F., Gerin M., Encrenaz P. J., Combes F., 1994, A&A, 287, 716  
 Chapman, S. C., Blain, A. W., Smail, I., Ivison, R. J., 2005, ApJ, 622, 772  
 Combes, Wiklind T., 1997, ApJ 486, L79  
 Combes, F., Maoli, R. & Omont, A., 1999, A&A, 345, 369  
 Danielson A., Swinbank, A., Smail, I. et al., 2010, MNRAS, arXiv1008.3183  
 Desert F-X., Boulanger F., Puget J-L.: 1990, A&A 237, 215  
 Encrenaz P., Combes F., Casoli F. et al.:1993, A&A, 273, L19  
 Gerin, M., Phillips T.G.: 2000, ApJ 537, 644  
 Greve, T.R., Bertoldi, F., Smail, I. et al.: 2005, MNRAS, 359, 1165  
 Greve, T.R., Pope A., Scott D. et al, 2008, MNRAS, 389, 1489  
 Hinshaw G., Weiland J.L., Hill R.S. et al: 2009, ApJS 180, 225  
 Imanishi, M., Nakanishi, K., Kuno, N., Kohno, K.: 2004, AJ 128, 2037  
 Iono, D., Wilson, C. D., Yun, M.S. et al: 2009, ApJ, 695, 1537  
 Kennicutt, R.: 1998, ARAA 38, 189  
 Kreysa, E., Gemuend, H.P., Gromke, J. et al. 1998, SPIE, 3357, 319  
 Lestrade, J-F, Wyatt M.C, Bertoldi F. et al, 2009, A&A, 506, 145  
 Pety, J., Beelen, A., Cox, P. et al.: 2004, A&A 428, L21  
 Riechers D.A., Weiss A., Walter F. et al. : 2006, ApJ 649, 635  
 Riechers D.A., Walter F., Bertoldi F. et al: 2009, ApJ 703, 1398  
 Riechers D.A., Capak P.L., Carilli C. et al: 2010, ApJ, 720, 431 press  
 Smail, I, Ivison, R.J., Blain, A.W., 1997, ApJ, 490, L5  
 Smail, I, Ivison, R.J., Blain, A.W., & Kneib, J.P., 2002, MNRAS, 331, 495  
 Solomon P.M., Downes D., Radford S. J. E., Barrett, J. W.: 1997, ApJ 478, 144  
 Tacconi L.J., Neri R., Chapman S.C. et al: 2006, ApJ 640, 228  
 van der Werf P., Isaak K., Meijerink R. et al.: 2010, A&A 518, L42  
 Vieira J.D., Crawford T.M., Switzer E.R. et al, 2010, ApJ 719, 763  
 Wagg J., Wilner, D. J., Neri, R., Downes, D., Wiklind, T.: 2006, ApJ 651, 46  
 Wardlow J.L., Smail I., Coppin K.E.K. et al.: 2010, MNRAS, arXiv: 1006.2137  
 Weiss A., Henkel C., Downes D., Walter F.: 2003, A&A, 409, L41  
 Weiss A., Downes D., Henkel, C., Walter F.: 2005, A&A, 429, L25  
 Weiss A., Downes D., Neri R., et al: 2007, A&A 467, 955  
 Weiss A., Ivison R.J., Downes D. et al, 2009, ApJ, 705, L45